

Long-term effects of retinopathy of prematurity (ROP) on rod and rod-driven function

Maureen E. Harris · Anne Moskowitz ·
Anne B. Fulton · Ronald M. Hansen

Received: 18 August 2010 / Accepted: 11 October 2010 / Published online: 3 November 2010
© Springer-Verlag 2010

Abstract The purpose of this study was to determine whether recovery of scotopic sensitivity occurs in human ROP, as it does in the rat models of ROP. Following a cross-sectional design, scotopic electroretinographic (ERG) responses to full-field stimuli were recorded from 85 subjects with a history of preterm birth. In 39 of these subjects, dark adapted visual threshold was also measured. Subjects were tested post-term as infants (median age 2.5 months) or at older ages (median age 10.5 years) and stratified by severity of ROP: severe, mild, or none. Rod photoreceptor sensitivity, S_{ROD} , was derived from the a-wave, and post-receptor sensitivity, $\log \sigma$, was calculated from the b-wave stimulus–response function. Dark adapted visual threshold was measured using a forced-choice preferential procedure. For S_{ROD} , the deficit from normal for age varied significantly with ROP severity but not with age group. For $\log \sigma$, in mild ROP, the deficit was smaller in older subjects than in infants, while in severe ROP, the deficit was quite large in both age groups. In subjects who never had ROP, S_{ROD} and $\log \sigma$ in both age groups were similar to those in term born controls. Deficits in dark adapted threshold and $\log \sigma$ were correlated in mild but not in severe ROP.

The data are evidence that sensitivity of the post-receptor retina improves in those with a history of mild ROP. We speculate that beneficial reorganization of the post-receptor neural circuitry occurs in mild but not in severe ROP.

Keywords Retinopathy of prematurity · Neural retina · Electroretinogram · Rod photoreceptor · Dark adapted visual threshold

Introduction

Retinopathy of prematurity (ROP), even if mild, causes long-term deficits in rod and rod-driven post-receptor retinal function that persist long after acute-phase ROP has resolved. Compared to term born controls, in the majority of ROP subjects, both rod photoreceptor and post-receptor response parameters are below average from early infancy into adulthood; former preterms who never had ROP do not differ from age-similar controls [1]. Rod and post-receptor retinal dysfunction are also noted in rat models of ROP [2–9]. In rats followed longitudinally, post-receptor sensitivity recovers whereas photoreceptor sensitivity remains abnormal [2].

To determine whether there is evidence of recovery of sensitivity in human ROP, we reviewed rod photoreceptor and post-receptor ERG parameters in infants and older subjects with a history of preterm

M. E. Harris · A. Moskowitz (✉) · A. B. Fulton ·
R. M. Hansen
Department of Ophthalmology, Children’s Hospital
and Harvard Medical School, 300 Longwood Avenue,
Boston, MA 02115, USA
e-mail: anne.moskowitz@childrens.harvard.edu

birth. Dark adapted visual thresholds were also evaluated for significant relationship to ERG indices of sensitivity. The effects of age and ROP severity on these cross-sectional ERG and threshold data from infant and older subjects were analyzed.

Methods

Subjects

Rod and rod-driven ERG parameters from 85 subjects with a history of preterm birth were analyzed (Table 1A). Peripheral dark adapted visual thresholds obtained from 39 of these subjects were also analyzed (Table 1B). ERG parameters from 68 of the subjects [1] and threshold data from 11 [10] have been reported previously.

All subjects had serial fundus examinations in the newborn intensive care nursery similar to those used in the multicenter ROP treatment trials [11, 12]. Based on these examinations, the subjects were categorized according to maximum acute-phase ROP as severe, treated ROP ($n = 14$), mild, untreated ROP ($n = 50$), or no ROP ($n = 21$) [13, 14]. Those in the severe category were treated by ablation of avascular

peripheral retina. Those in the mild category did not require treatment; by clinical criteria, their ROP resolved completely. Those in the no ROP category had serial examinations and ROP was never detected. No subject had active ROP at the time of the ERG test and none had a history of retinal detachment or surgery other than laser or cryotherapy.

Gestational age at birth ranged from 23 to 32 (median 27) weeks and birth weight from 490 to 2,275 (median 845) grams (Table 1A). Although, on average, those with severe ROP were born earlier and had lower birth weights, there was considerable overlap in gestational age at birth and birth weight among the three groups.

The 85 subjects were stratified into two age groups: infant and older (Table 1A). Infants ($n = 35$) were tested at median age 10.3 (range 7.4–36.3) weeks post-term. Older subjects ($n = 50$) were tested at median age 10.5 (range 3.1–23.0) years post-term. The demographics of the subset with dark adapted visual thresholds are summarized in Table 1B. Throughout this paper, we report the age of former preterm subjects as post-term age. Post-term age is calculated by subtracting the difference between the gestational age at birth and full term (40 weeks) from the subject's postnatal age: Post-term age = Postnatal

Table 1 Former preterm subjects [median (range)]

Category	<i>n</i>	Gestational age (weeks)	Birth weight (g)	Age at test (post-term)
<i>A. ERG subjects</i>				
Infants ($n = 35$)				
Severe ROP	5	27.0 (25–28)	950 (499–1,040)	11.6 (9.0–31.3) weeks
Mild ROP	21	27.0 (24–31)	890 (610–1,332)	10.3 (7.4–36.3) weeks
No ROP	9	29.0 (25–32)	1,270 (740–2,275)	10.3 (9.1–33.8) weeks
Older ($n = 50$)				
Severe ROP	9	26.0 (24–30)	634 (490–1,750)	10.0 (5.9–18.5) years
Mild ROP	29	25.0 (23–32)	760 (500–1,588)	11.1 (3.1–23.0) years
No ROP	12	30.5 (26–32)	1,424 (820–2,268)	9.8 (3.1–18.1) years
<i>B. Subset of ERG subjects with dark adapted visual thresholds</i>				
Infants ($n = 20$)				
Severe ROP	5	27.0 (25–28)	950 (499–1,040)	11.7 (9.4–32.9) weeks
Mild ROP	11	28.0 (24–30)	940 (610–1,230)	10.7 (7.6–18.9) weeks
No ROP	4	28.0 (27–30)	1,250 (1,195–1,270)	10.5 (9.9–11.3) weeks
Older ($n = 19$)				
Severe ROP	4	25.5 (24–28)	634 (490–1,100)	10.4 (6.7–14.5) years
Mild ROP	12	25.5 (24–32)	785 (595–1,588)	11.6 (3.1–14.9) years
No ROP	3	26.0 (26–30)	930 (820–1,400)	7.7 (3.0–13.9) years

age – (Term – Gestational age). For example, the post-term age of an infant born at 26-week gestation and tested at postnatal age 24 weeks is 10 weeks [24 – (40 – 26) = 10].

This study conformed to the tenets of the Declaration of Helsinki and was approved by the Children’s Hospital Committee on Clinical Investigation. Informed consent was obtained from the parents of the infants and children, assent from the older children, and consent from those 18 years and older.

ERG procedure

The majority of preterm subjects (70/85; 82%) were tested with Burian-Allen corneal contact electrodes. Skin electrodes were used in 15 of the 50 older preterm subjects who were judged unlikely to tolerate the Burian-Allen electrode. The skin electrode subjects were median age 6.9 (range 3.0–11.9) years and were distributed across ROP strata (severe: $n = 3$, mild: $n = 9$, no ROP: $n = 3$). ERGs from preterms were compared to those from term born 10-week-old infants ($n = 38$) and mature ($n = 60$) subjects [1]. All controls were tested with Burian-Allen electrodes; 18 of the mature controls were also tested using skin electrodes.

Parents stayed with infants and children throughout the procedure. One pupil was dilated with cyclopentolate 1% and the subject was dark-adapted for 30 min. Then, under dim red light, proparacaine 0.5% was instilled and a bipolar Burian-Allen electrode was placed on the cornea. For skin electrode testing, the active electrode was placed near the outer canthus and the indifferent electrode below the lower lid [15]. For both electrode types, a ground electrode was placed on the skin over the ipsilateral mastoid.

A Compact 4 system (Nicolet, Madison, WI) was used to test 55 and an Espion system (Diagnosys, Lowell, MA) was used to test 30 of the former preterm subjects. Rod responses were recorded using a Wratten 47B filter ($\lambda < 510$ nm) in the Nicolet system and a 470-nm LED (half bandwidth 30 nm) in the Espion system. In both systems, the gain was 1,000 and the bandpass was 0.5–1,000 Hz. The digitization rate was 2,564 Hz for the Nicolet and 2,000 Hz for the Espion. In the adult control subjects (Nicolet: $n = 28$; Espion: $n = 32$), rod photoreceptor and post-receptor parameters did not differ between the two recording

systems. Therefore, data obtained using the two systems have been combined in all analyses.

Rod photoreceptor

The activation of phototransduction was studied in all subjects. Responses to full-field, brief (<3 ms), blue stimuli ranging from +2.1 to +3.6 log scot td s were recorded. The rod photoresponse parameters (S_{ROD} and R_{ROD}) were calculated by fit of the Hood and Birch [16] formulation of the Lamb and Pugh model [17, 18] to the a-waves. The equation is

$$R(i, t) = [1 - \exp\{-0.5 I S_{\text{ROD}}(t - t_d)^2\}] R_{\text{ROD}} \quad (1)$$

where I is the flash (scot td s), S_{ROD} , a parameter [(scot td) $^{-1}$ s $^{-3}$] that depends on the time constants of the steps in the activation of phototransduction [18], R_{ROD} , the saturated response amplitude (μV), and t_d , a brief delay (ms). All three parameters (S_{ROD} , R_{ROD} , and t_d) were free to vary.

Post-receptor rod-driven b-wave

The stimulus/response function

$$V(I) = [I/(I + \sigma)] V_{\text{MAX}} \quad (2)$$

was fit to the b-wave amplitudes of each subject. In this equation, V is the b-wave amplitude (μV) produced by flash intensity I , V_{MAX} the saturated amplitude (μV), I the stimulus in scot td s, and σ the stimulus that evokes a half-maximum b-wave amplitude. Thus, $1/\sigma$ is a measure of sensitivity.

The function was fit only up to those higher intensities at which substantial a-wave intrusion occurred ($\sim +1.0$ log scot td s) [19]. Under these rod-mediated conditions, the b-wave represents the activity of ON bipolar and other second- and third-order neurons [20, 21].

Validation of parameters obtained using skin electrodes

In a preliminary analysis, we tested adult, term born control subjects ($n = 18$) with both the Burian-Allen electrode and skin electrodes (Table 2). There was no significant difference (repeated measures t test) in the estimates of S_{ROD} or $\log \sigma$, but skin electrode amplitudes (R_{ROD} and V_{MAX}) were significantly smaller than Burian-Allen amplitudes. In an

Table 2 Comparison of Burian-Allen and skin electrode results in mature, term born controls [median (range)]

	Rod photoreceptor		Post-receptor	
	S_{ROD} (scot td s)	R_{ROD} (μV)	Log σ (scot td s)	V_{MAX} (μV)
Burian-Allen	84.9 (53.6–110.5)	395 (137–541)	−0.8 (−1.1–−0.2)	431 (305–566)
Skin	73.0 (12.8–123.8)	58 (17–97)	−0.8 (−1.2–−0.1)	72 (42–115)

individual, the difference between Burian-Allen and skin electrode estimates of both S_{ROD} and log σ was small. Specifically, the median difference in log S_{ROD} was +0.04 (range −0.24–+0.17 log unit), and the median difference in log σ was +0.02 (range −0.19–+0.40 log unit). Thus, S_{ROD} and log σ parameters obtained with skin and Burian-Allen electrodes were combined. For every individual, saturated amplitudes (R_{ROD} and V_{MAX}) obtained with skin electrodes were considerably smaller than those obtained with the Burian-Allen electrode [R_{ROD} : median 16% (range 6–31%); V_{MAX} : median 16% (range 11–34%)].

Psychophysical thresholds

Peripheral visual thresholds were estimated using a two-alternative, forced-choice method, as previously described [22]. After dark adapting for 30 min, the subject was positioned in front of a rear projection screen. A 30 minarc diameter, flickering, red light attracted the subject's gaze to the center of the screen. When an adult observer reported that the subject was looking at the center, the fixation target was extinguished and a peripheral test stimulus presented. Stimuli were 50-ms duration, blue (Wratten 47B, $\lambda < 510$ nm), 2° diameter spots presented 30° to the right or left of the fixation target. Stimulus intensity was controlled using calibrated neutral density filters. The observer, unaware of the right–left position of the test stimulus, reported stimulus location, right or left, based on the subject's head and eye movements. Older subjects pointed to the stimulus or reported its location verbally. Thresholds were determined using a transformed up-down staircase that estimated the 70.7% correct point of the psychometric function [23].

Calibrations

Stimuli were measured with a detector and appropriate scotopic filter (IL 1700, International Light, Newburyport, MA) placed at the position of the subject's cornea. The maximum intensity stimulus

was 79.2 scotopic cd/m^2 in the ERG system and 5.0 scotopic cd/m^2 in the psychophysical apparatus. In adults, assuming a pupil diameter of 8 mm, the ERG stimulus produced approximately +3.6 log scot td s and the psychophysical stimulus approximately +2.4 log scot td s. In our analysis of rod photoreceptor and post-receptor function, we used the same troland values for both infant and older subjects.

Retinal illuminance varies directly with area of the pupil and transmissivity of the ocular media and inversely with the square of the posterior nodal distance [24, 25]. The infants' median pupil diameter was 5.0 mm. We used the area of each infants' dilated pupil and published estimates of the ocular media density [26] and axial length of the eye [27] to estimate the retinal illuminance. In summary, equal intensity stimuli produce retinal illuminance in 10-week-old infants which differs from that in older subjects by less than 0.1 log unit [1, 28–30]. For the ERG system, the maximum stimulus was 6.13 lm/m^2 ; for the psychophysical apparatus, it was 0.44 lm/m^2 .

Statistical analyses

For each subject, ERG parameters (S_{ROD} , log σ , R_{ROD} , and V_{MAX}) were expressed as the log of the difference from the calculated normal value for age [31]. In normal development, these parameters do not change significantly after infancy [31].

Analysis of variance (ANOVA) was used to evaluate the effect of ROP severity (severe, mild, no ROP) and age (infant, older) on each ERG parameter. All ANOVA results are summarized in Table 3.

For those subjects who had dark adapted visual threshold measured, linear regression was used to compare deficit in threshold for significant relationship to deficit in photoreceptor (S_{ROD}) and post-receptor (log σ) sensitivity. Thresholds and ERG parameters were expressed as difference from mean adult control values [31].

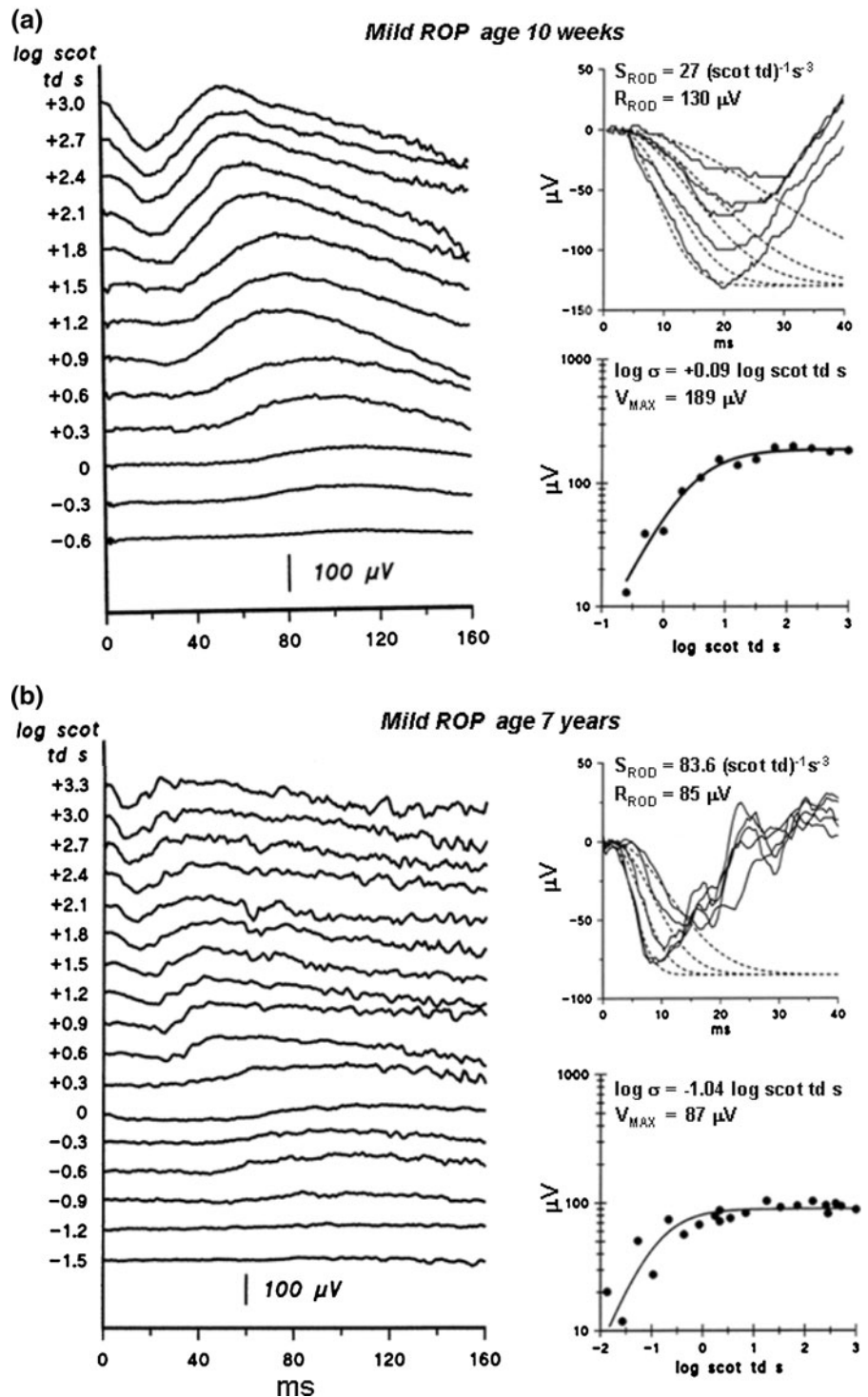
The level of significance for all tests was $P \leq 0.01$.

Results

Sample ERG records (Fig. 1) from two mild ROP subjects are shown, one recorded using a

Burian-Allen electrode, the other recorded with skin electrodes. Model fits to the a-wave, and the b-wave stimulus response functions are also shown.

Fig. 1 Sample ERG records from mild ROP subjects. **a** ERGs recorded using a Burian-Allen contact electrode and model fits to a- and b-waves in a 10-week-old infant with a history of mild ROP. *Left:* Dark adapted ERG responses to a series of flashes. Flash intensity in log scot td s is indicated to the left of the traces. *Upper right:* The first 40 ms of the response (*solid lines*) to the five brightest flashes and model fits to the a-wave (Eq. 1, *dashed lines*). The calculated values of S_{ROD} and R_{ROD} are indicated. *Lower right:* b-wave amplitude plotted as a function of stimulus intensity. The smooth curve represents Eq. 2 fit to the points. The calculated values of $\log \sigma$ and V_{MAX} are indicated. **b** ERGs recorded using skin electrodes in a 7-year-old child with a history of mild ROP. The features are the same as in **a**



Mean values of sensitivity parameters S_{ROD} and $\log \sigma$ expressed as the log of the difference from normal for age ($\Delta \log$ normal) are shown for each ROP category and age group in Fig. 2. ANOVA (Table 3) showed that deficits in $\log S_{\text{ROD}}$ (upper panel) varied significantly with ROP severity but not with age. On average, the S_{ROD} deficit in the severe category was 0.38 log unit (infant) and 0.32 log unit (older), that is, sensitivity was 42 and 48% of that in the controls. In those with mild ROP, the S_{ROD} deficit was smaller: 0.22 log unit (infant) and 0.12 log unit (older), that is, sensitivity was 60 and 76% of that in controls. For those with no ROP, S_{ROD} was normal at both ages.

Deficits in post-receptor sensitivity are summarized in Fig. 2, lower panel. The deficit in $\log \sigma$ varied significantly with ROP severity but not with age (Table 3). Of note, there was a significant interaction between age and ROP severity. In subjects with a history of mild ROP, the deficit in $\log \sigma$ was significantly smaller in the older group than in the infant group ($t = 6.74$; $df = 79$; $P < 0.01$), while in subjects with a history of severe ROP, large deficits

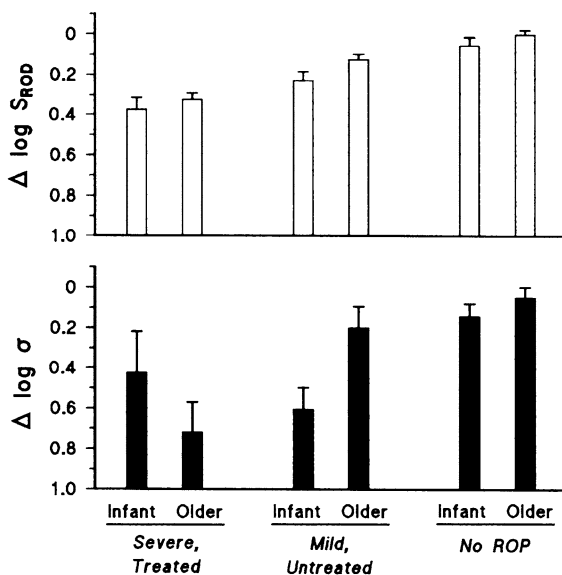


Fig. 2 Mean (SEM) sensitivity expressed as the log of the difference from normal for age ($\Delta \log$ normal). *Upper panel:* Rod photoreceptor sensitivity, S_{ROD} . In both mild and severe ROP, significant deficits in S_{ROD} were seen in infants and older subjects. *Lower panel:* Rod post-receptor sensitivity, $\log \sigma$. In infants, $\log \sigma$ was low in those with a history of ROP, whether mild or severe. In older subjects, deficits in $\log \sigma$ were smaller in mild than in severe ROP

were found in both age groups; the latter deficits were not significantly different.

Deficits in rod photoreceptor and post-receptor saturated amplitude (R_{ROD} and V_{MAX} , respectively) are summarized in Fig. 3. The deficits in both $\log R_{\text{ROD}}$ and $\log V_{\text{MAX}}$ varied significantly with severity but not with age (Table 3). Both amplitude parameters were lowest in severe ROP. There was no significant interaction between age and ROP severity for either amplitude parameter.

Deficit in peripheral dark adapted visual threshold is plotted as a function of deficit in post-receptor sensitivity in Fig. 4. In the no ROP subjects (upper panel), as in normal development, the deficit in psychophysical threshold was predicted by the deficit in $\log \sigma$. In mild ROP (center panel), deficits in $\log \sigma$ and peripheral threshold were similar; the points fell near the diagonal line (slope = 1.0) that indicates equal deficits in both. There was a significant relationship between deficit in threshold and deficit in $\log \sigma$ ($y = 0.44x - 11$; $r = 0.46$; $t = 3.50$; $P < 0.001$). The slope of the regression line did not differ significantly from 1.0. In severe ROP (lower panel), there was no relationship between deficit in threshold and deficit in $\log \sigma$.

In normal development, photoreceptor sensitivity (S_{ROD}) predicts dark adapted visual threshold elevation [32]. In ROP, whether mild or severe, there was no significant relationship between S_{ROD} and threshold (not shown). The relationship in subjects

Table 3 Results of analyses of variance

	Sensitivity ($\Delta \log$ normal for age)					
	Photoreceptor (S_{ROD})			Post-receptor ($\log \sigma$)		
	<i>F</i>	<i>df</i>	<i>P</i>	<i>F</i>	<i>df</i>	<i>P</i>
Severity	19.31	2, 79	<0.001	8.61	2, 79	<0.01
Age	3.04	1, 79	ns	0.47	1, 79	ns
Age \times Severity	0.30	2, 79	ns	5.32	2, 79	<0.01
	Saturated Amplitude ($\Delta \log$ normal for age)					
	Photoreceptor (R_{ROD})			Post-receptor (V_{MAX})		
	<i>F</i>	<i>df</i>	<i>P</i>	<i>F</i>	<i>df</i>	<i>P</i>
Severity	5.09	2, 79	<0.01	7.89	2, 79	<0.01
Age	3.75	1, 79	ns	0.64	1, 79	ns
Age \times Severity	0.64	2, 79	ns	0.09	2, 79	ns

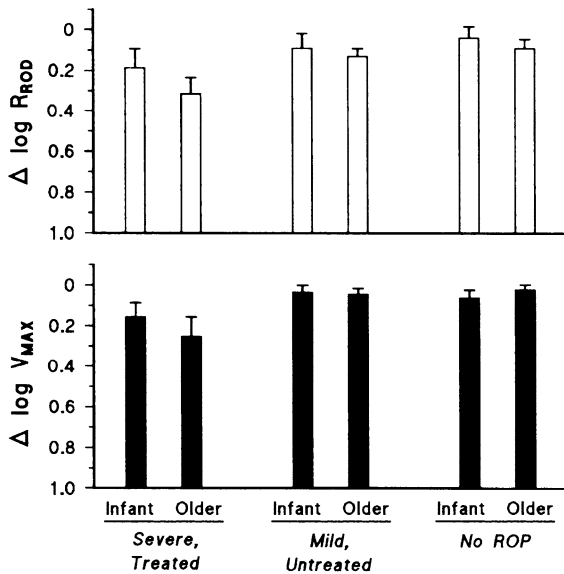


Fig. 3 Mean (SEM) saturated amplitude expressed as the log of the difference from normal for age ($\Delta \log$ normal). *Upper panel*: Rod photoreceptor saturated amplitude, R_{ROD} . *Lower panel*: Post-receptor saturated amplitude, V_{MAX} . The deficit in both amplitude parameters was greatest in severe ROP

with no ROP was similar to that in normal development.

Discussion

Small but statistically significant deficits in rod photoreceptor sensitivity, S_{ROD} , are seen in both infants and older subjects with a history of mild and severe ROP (Fig. 2, upper panel). Photoreceptors appear to be a therapeutic target in ROP. Pharmacological protection of immature photoreceptors benefits the neurovascular outcome in a rat model of ROP [33].

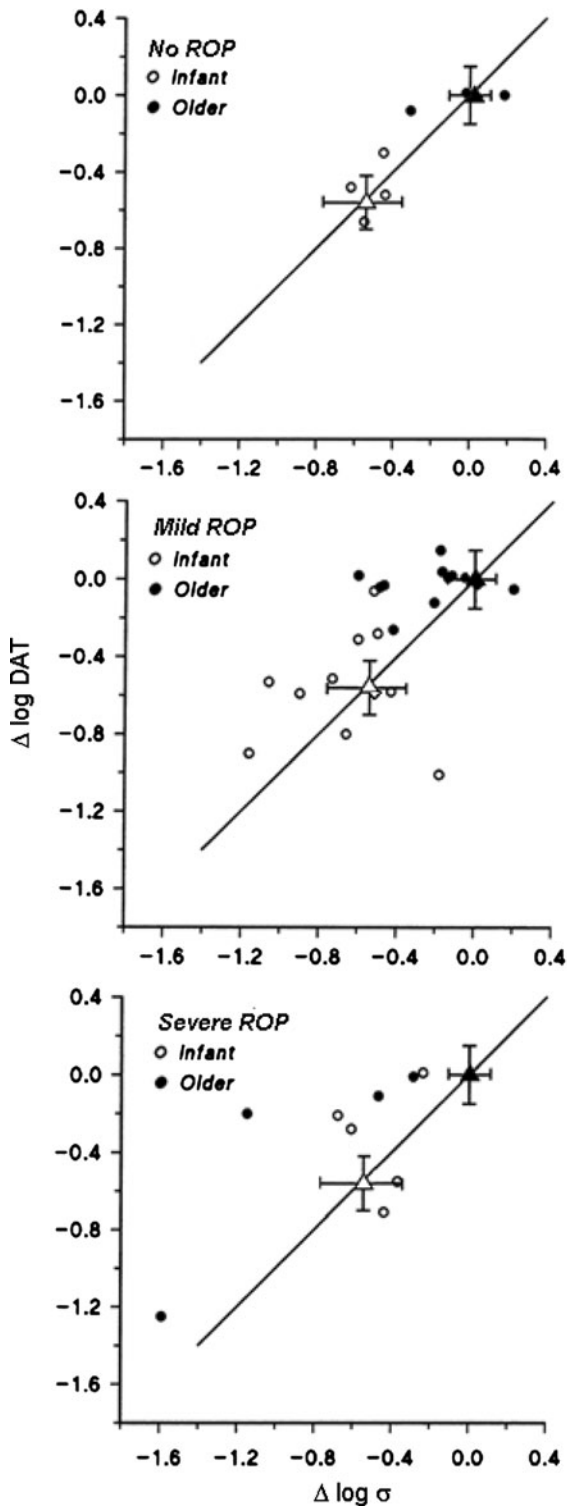
Deficits in post-receptor sensitivity, represented by $\log \sigma$, are seen in infants with a history of mild and severe ROP. In older subjects, the $\log \sigma$ deficits are minimal in mild ROP but marked in severe ROP (Fig. 2, lower panel). These cross-sectional ERG data from young infants and older subjects (>3 years) suggest that in mild ROP, post-receptor sensitivity improves after early infancy. In mild ROP, deficits in post-receptor sensitivity and deficits in threshold are correlated (Fig. 4, middle panel). Our previous longitudinal psychophysical measures of dark adapted visual threshold [10] indicated that

in mild ROP, peripheral retinal sensitivity reached maturity in late infancy (9–12 months post-term). Therefore, we predict that post-receptor sensitivity ($\log \sigma$) also matures in late infancy. In term born controls, peripheral sensitivity is mature by age 6 months [22].

We hypothesize that in mild ROP patients, beneficial reorganization (“rewiring”) of post-receptor retinal circuitry leads not only to improved ERG sensitivity but also to normal visual thresholds [10]. We have previously observed beneficial reorganization in a patient with desferoxamine toxicity [34] whom we have now followed for more than a decade. Pharmacological exposure caused photoreceptor, post-receptor, and visual dysfunction. Mild rod dysfunction (S_{ROD}) was irreversible but post-receptor function ($\log \sigma$) and visual threshold recovered [34]. In animals, more severe injury to the photoreceptors, due to light damage or heritable degeneration, causes marked detrimental remodeling of the post-receptor retina [35–37]. We suspect that in mild human ROP, stepwise beneficial remodeling of neural and vascular elements occurs. Growth factors mediate neural-vascular cross talk during the evolution and resolution of ROP in a rat model [38]. Analogous processes may be operative in human ROP.

The apparent lack of post-receptor recovery in severe ROP could be consequent to the intimate relationship between the post-receptor neural retina and its vascular supply. By definition, acute vascular abnormalities are more marked in severe than in mild ROP and may be associated with irreparable injury to the post-receptor neural circuitry. We cannot exclude the possibility that in some patients with severe ROP, the post-receptor circuitry recovers by late infancy only to lose function in childhood. We have, however, found no evidence of this in the extant data (Fig. 2, lower panel).

Further delineation of the interplay of the post-receptor neural circuitry and the retinal vasculature is essential for understanding of the recovery of function in mild ROP and the apparent lack of recovery in severe ROP. Such understanding may lead to improved clinical outcomes, perhaps by identifying new therapeutic targets. Complementary analyses of vasculature and retinal layer morphology [39–41] and of function, assessed using ERG and psychophysical methods, will provide the critical information in infants and children. Interpretation of the retinal



◀ **Fig. 4** Deficit in dark adapted peripheral threshold ($\Delta \log \text{DAT}$) plotted as a function of deficit in post-receptor sensitivity ($\Delta \log \sigma$) in preterm subjects with a history of no ROP (*top*), mild ROP (*middle*), and severe ROP (*bottom*). The circles represent data from individual preterm subjects (*open circles*—infants; *filled circles*—older subjects). The triangles indicate the mean ($\pm \text{SEM}$) for term born 10-week-old infants (*open*) and adults (*filled*). The mean normal adult value is at coordinates (0,0). The *solid line* has a slope of 1

Acknowledgments This work was supported by National Eye Institute Grant R01 EY010597.

References

1. Fulton AB, Hansen RM, Moskowitz A, Akula JD (2009) The neurovascular retina in retinopathy of prematurity. *Prog Retin Eye Res* 28:452–482 Corrigendum 2010;29:94
2. Akula JD, Hansen RM, Martinez-Perez ME, Fulton AB (2007) Rod photoreceptor function predicts blood vessel abnormality in retinopathy of prematurity. *Invest Ophthalmol Vis Sci* 48:4351–4359
3. Akula JD, Mocko JA, Moskowitz A, Hansen RM, Fulton AB (2007) The oscillatory potentials of the dark-adapted electroretinogram in retinopathy of prematurity. *Invest Ophthalmol Vis Sci* 48:5788–5797
4. Liu K, Akula JD, Falk C, Hansen RM, Fulton AB (2006) The retinal vasculature and function of the neural retina in a rat model of retinopathy of prematurity. *Invest Ophthalmol Vis Sci* 47:2639–2647
5. Liu K, Akula JD, Hansen RM, Moskowitz A, Kleinman MS, Fulton AB (2006) Development of the electroretinographic oscillatory potentials in normal and ROP rats. *Invest Ophthalmol Vis Sci* 47:5447–5452
6. Dembinska O, Rojas LM, Chemtob S, Lachapelle P (2002) Evidence for a brief period of enhanced oxygen susceptibility in the rat model of oxygen-induced retinopathy. *Invest Ophthalmol Vis Sci* 43:2481–2490
7. Dembinska O, Rojas LM, Varma DR, Chemtob S, Lachapelle P (2001) Graded contribution of retinal maturation to the development of oxygen-induced retinopathy in rats. *Invest Ophthalmol Vis Sci* 42:1111–1118
8. Dorfman AL, Chemtob S, Lachapelle P (2010) Postnatal hyperoxia and the developing rat retina: beyond the obvious vasculopathy. *Doc Ophthalmol* 120:61–66
9. Fletcher EL, Downie LE, Hatzopoulos K, Vessey KA, Ward MM, Chow CL, Pianta MJ, Vingrys AJ, Kalloniatis M, Wilkinson-Berka JL (2010) The significance of neuronal and glial cell changes in the rat retina during oxygen-induced retinopathy. *Doc Ophthalmol* 120:67–86
10. Barnaby AM, Hansen RM, Moskowitz A, Fulton AB (2007) Development of scotopic visual thresholds in retinopathy of prematurity. *Invest Ophthalmol Vis Sci* 48:4854–4860
11. Cryotherapy for Retinopathy of Prematurity Cooperative Group (1988) Multicenter trial of cryotherapy for

processes in human ROP will undoubtedly continue to be informed by the results of investigations in rat models [2, 33, 38, 42–45].

- retinopathy of prematurity. Preliminary results Arch Ophthalmol 106:471–479
12. Hardy RJ, Good WV, Dobson V, Palmer EA, Phelps DL, Quintos M, Tung B (2004) Multicenter trial of early treatment for retinopathy of prematurity: study design. *Control Clin Trials* 25:311–325
 13. International Committee for the Classification of Retinopathy of Prematurity (2005) The international classification of retinopathy of prematurity revisited. *Arch Ophthalmol* 123:991–999
 14. Early Treatment for Retinopathy of Prematurity Cooperative Group (2003) Revised indications for the treatment of retinopathy of prematurity: results of the early treatment for retinopathy of prematurity randomized trial. *Arch Ophthalmol* 121:1684–1694
 15. Bradshaw K, Hansen R, Fulton A (2004) Comparison of ERGs recorded with skin and corneal-contact electrodes in normal children and adults. *Doc Ophthalmol* 109:43–55
 16. Hood DC, Birch DG (1994) Rod phototransduction in retinitis pigmentosa: estimation and interpretation of parameters derived from the rod a-wave. *Invest Ophthalmol Vis Sci* 35:2948–2961
 17. Lamb TD, Pugh EN Jr (1992) A quantitative account of the activation steps involved in phototransduction in amphibian photoreceptors. *J Physiol* 449:719–758
 18. Pugh EN Jr, Lamb TD (1993) Amplification and kinetics of the activation steps in phototransduction. *Biochim Biophys Acta* 1141:111–149
 19. Peachey NS, Alexander KR, Derlacki DJ, Fishman GA (1992) Light adaptation and the luminance-response function of the cone electroretinogram. *Doc Ophthalmol* 79:363–369
 20. Aleman TS, LaVail MM, Montemayor R, Ying G, Maguire MM, Laties AM, Jacobson SG, Cideciyan AV (2001) Augmented rod bipolar cell function in partial receptor loss: an ERG study in P23H rhodopsin transgenic and aging normal rats. *Vision Res* 41:2779–2797
 21. Wurzig K, Lichtenberger T, Hanitzsch R (2001) On-bipolar cells and depolarising third-order neurons as the origin of the ERG-b-wave in the RCS rat. *Vision Res* 41:1091–1101
 22. Hansen RM, Fulton AB (1999) The course of maturation of rod-mediated visual thresholds in infants. *Invest Ophthalmol Vis Sci* 40:1883–1886
 23. Wetherill GB, Levitt H (1965) Sequential estimation of points on a psychometric function. *Br J Math Stat Psychol* 18:1–10
 24. Pugh EN Jr. (1988) Vision: physical and retinal physiology. In: Atkinson RC, et al. (Eds) *Stevens handbook of experimental psychology*, vol 1, Perception and motivation, 2nd edn. Wiley, New York. pp 75–163
 25. McCulloch DL, Hamilton R (2010) Essentials of photometry for clinical electrophysiology of vision. *Doc Ophthalmol* 121:77–84
 26. Hansen RM, Fulton AB (1989) Psychophysical estimates of ocular media density of human infants. *Vision Res* 29:687–690
 27. Mactier H, Maroo S, Bradnam M, Hamilton R (2008) Ocular biometry in preterm infants: implications for estimation of retinal illuminance. *Invest Ophthalmol Vis Sci* 49:453–457
 28. Brown AM, Dobson V, Maier J (1987) Visual acuity of human infants at scotopic, mesopic and photopic luminances. *Vision Res* 27:1845–1858
 29. Hansen RM, Fulton AB (2005) Recovery of the rod photo-response in infants. *Invest Ophthalmol Vis Sci* 46:764–768
 30. Malcolm CA, Hamilton R, McCulloch DL, Montgomery C, Weaver LT (2003) Scotopic electroretinogram in term infants born of mothers supplemented with docosahexaenoic acid during pregnancy. *Invest Ophthalmol Vis Sci* 44:3685–3691
 31. Fulton AB, Hansen RM (2000) The development of scotopic sensitivity. *Invest Ophthalmol Vis Sci* 41:1588–1596
 32. Hansen RM, Fulton AB (1995) The VEP thresholds for full-field stimuli in dark-adapted infants. *Vis Neurosci* 12:223–228
 33. Akula JD, Favazza TL, Mocko JA, Benador IY, Asturias AL, Kleinman MS, Hansen RM, Fulton AB (2010) The anatomy of the rat eye with oxygen-induced retinopathy. *Doc Ophthalmol* 120:41–50
 34. Lu M, Hansen RM, Cunningham MJ, Eklund SE, Fulton AB (2007) Effects of desferoxamine on retinal and visual function. *Arch Ophthalmol* 125:1581–1582
 35. Marc RE, Jones BW (2003) Retinal remodeling in inherited photoreceptor degenerations. *Mol Neurobiol* 28:139–147
 36. Marc RE, Jones BW, Watt CB, Strettoi E (2003) Neural remodeling in retinal degeneration. *Prog Retin Eye Res* 22:607–655
 37. Marc RE, Jones BW, Watt CB, Vazquez-Chona F, Vaughan DK, Organisciak DT (2008) Extreme retinal remodeling triggered by light damage: implications for age related macular degeneration. *Mol Vis* 14:782–806
 38. Akula JD, Mocko JA, Benador IY, Hansen RM, Favazza TL, Vyhovsky TC, Fulton AB (2008) The neurovascular relation in oxygen-induced retinopathy. *Mol Vis* 14:2499–2508
 39. Gelman R, Martinez-Perez ME, Vanderveen DK, Moskowitz A, Fulton AB (2005) Diagnosis of plus disease in retinopathy of prematurity using Retinal image multiScale analysis. *Invest Ophthalmol Vis Sci* 46:4734–4738
 40. Wilson CM, Cocker KD, Moseley MJ, Paterson C, Clay ST, Schulenburg WE, Mills MD, Ells AL, Parker KH, Quinn GE, Fielder ARNG J (2008) Computerized analysis of retinal vessel width and tortuosity in premature infants. *Invest Ophthalmol Vis Sci* 49:3577–3585
 41. Hammer DX, Ifimia NV, Ferguson RD, Bigelow CE, Ustun TE, Barnaby AM, Fulton AB (2008) Foveal fine structure in retinopathy of prematurity: an adaptive optics fourier domain optical coherence tomography study. *Invest Ophthalmol Vis Sci* 49:2061–2070
 42. Penn JS, Henry MM, Wall PT, Tolman BL (1995) The range of PaO₂ variation determines the severity of oxygen-induced retinopathy in newborn rats. *Invest Ophthalmol Vis Sci* 36:2063–2070
 43. Barnett JM, Yanni SE, Penn JS (2010) The development of the rat model of retinopathy of prematurity. *Doc Ophthalmol* 120:3–12
 44. Berkowitz BA, Roberts R (2010) Evidence for a critical role of panretinal pathophysiology in experimental ROP. *Doc Ophthalmol* 120:13–24
 45. Hartnett ME (2010) The effects of oxygen stresses on the development of features of severe retinopathy of prematurity: knowledge from the 50/10 OIR model. *Doc Ophthalmol* 120:25–39